

TrpM8-mediated somatosensation in mouse neocortex

Short title: Cortical representation of cold

Patrick Beukema², Katherine L. Cecil⁶, Elena Peterson, Victor R. Mann⁵, Megumi

Matsushita¹, Yoshio Takashima³, Saket Navlakha⁴, and Alison L. Barth¹

¹Department of Biological Sciences and Center for the Neural Basis of Cognition,
Carnegie Mellon University, 4400 Fifth Avenue, Pittsburgh PA 15213

²Center for Neuroscience at the University of Pittsburgh, Department of Neuroscience,
Pittsburgh PA 15260

³Department of Anesthesiology, University of California, San Diego, La Jolla, CA 92093

⁴Integrative Biology Laboratory, The Salk Institute for Biological Studies, La Jolla, CA
92037

⁵Dept of Chemistry, University of California, Berkeley, CA 94720

⁶Baylor College of Medicine, Houston, Texas, 77030

[^]Corresponding author

This article has been accepted for publication and undergone full peer review but has not been through the copyediting, typesetting, pagination and proofreading process which may lead to differences between this version and the Version of Record. Please cite this article as an 'Accepted Article', doi: 10.1002/cne.24418

© 2018 Wiley Periodicals, Inc.

Received: Sep 07, 2017; Revised: Feb 06, 2018; Accepted: 06 12, 2018

Abstract

Somatosensation is a complex sense mediated by more than a dozen distinct neural subtypes in the periphery. Although pressure and touch sensation have been mapped to primary somatosensory cortex in rodents, it has been controversial whether pain and temperature inputs are also directed to this area. Here we use a well-defined somatosensory modality, cool sensation mediated by peripheral TrpM8-receptors, to investigate the neural substrate for cool perception in the mouse neocortex. Using activation of cutaneous TrpM8 receptor-expressing neurons, we identify candidate neocortical areas responsive for cool sensation. Initially, we optimized TrpM8 stimulation and determined that menthol, a selective TrpM8 agonist, was more effective than cool stimulation at inducing expression of the immediate-early gene *c-fos* in the spinal cord. We developed a broad-scale brain survey method for identification of activated brain areas, using automated methods to quantify *c-fos* immunoreactivity (fos-IR) across animals. Brain areas corresponding to the posterior insular cortex and secondary somatosensory (S2) show elevated fos-IR after menthol stimulation, in contrast to weaker activation in primary somatosensory cortex (S1). In addition, menthol exposure triggered fos-IR in piriform cortex, the amygdala, and the hypothalamus. Menthol-mediated activation was absent in TrpM8-knock-out animals. Our results indicate that cool somatosensory input broadly drives neural activity across the mouse brain, with neocortical signal most elevated in the posterior insula, as well as S2 and S1. These findings are consistent with data from humans indicating that the posterior insula is specialized for somatosensory information encoding temperature, pain, and gentle touch.

Keywords: TrpM8, insula, somatosensation, pain, thermal sensation, *c-fos*, automated cell counting, cold, cool, menthol, RRID AB_2314421

Introduction

Different modalities of somatosensory information – light touch, pressure, vibration, pinprick touch, pain, and temperature – are distributed across specialized neuronal subtypes in the dorsal root ganglion, a segregation that is at least partly maintained in subsequent levels of processing, including the spinal cord (Craig, 2003; Y. Liu & Ma, 2011). However, the way these different streams of information are represented and integrated in the brain is unclear. Indeed, individual neurons in primary somatosensory cortex (S1) can respond to multiple forms of cutaneous stimulation (D. R. Kenshalo, Iwata, Sholas, & Thomas, 2000; Milenkovic et al., 2014), suggesting that fine distinctions at the periphery may not be maintained in the CNS, although perceptually different somatosensory qualities can be easily reported in humans. In addition to S1, at least four other somatosensory maps have been identified in both humans and other mammals (see for example (Kaas & Collins, 2003; Krubitzer & Calford, 1992)); these include secondary somatosensory cortex (S2) and the posterior insula. Rodents possess at least three of these somatosensory areas, including S1, S2, and a correlate of the posterior insula (Rodgers, Benison, Klein, & Barth, 2008). The distribution of different forms of somatosensory input across these cortical areas, and the way that sensory information is integrated and localized across areas, remains an open question. The first step in addressing this will be identifying specific neocortical areas or neurons that are activated by different somatosensory stimuli.

Multiple lines of evidence indicate that the insula is an important neocortical locus activated by cutaneous thermal stimulation in humans (Baier et al., 2014; Baumgartner et al., 2010; Birklein, Rolke, & Muller-Forell, 2005; Brooks, Zambreanu, Godinez, Craig, & Tracey, 2005; Casey, Minoshima, Morrow, & Koeppe, 1996; Craig, Chen, Bandy, & Reiman, 2000; Davis, Kwan, Crawley, & Mikulis, 1998; Davis, Pope, Crawley, & Mikulis,

2004; Egan et al., 2005; Greenspan, Ohara, Franaszczuk, Veldhuijzen, & Lenz, 2008; Greenspan & Winfield, 1992; Mazzola, Faillenot, Barral, Mauguiere, & Peyron, 2012; Stephani, Fernandez-Baca Vaca, Maciunas, Koubeissi, & Luders, 2011). In particular, the posterior insula has been linked to non-noxious cold sensation: fMRI, PET, and evoked potential studies show somatotopic activation in this region, with hand and forearm representations lying anterior to foot and leg (Craig, et al., 2000; Davis, et al., 1998; Egan, et al., 2005; Greenspan, et al., 2008). In one case study, an individual with a well-defined focal lesion in the posterior insula had a complete loss of cold sensation in the hand and arm, consistent with cold-specialization and somatotopy of this region (Birklein, et al., 2005), and another individual with a tumor in the insula reported a change in cold-detection thresholds (Greenspan & Winfield, 1992).

Sophisticated molecular genetic tools and cellular recording techniques in rodents greatly facilitate studies to understand somatosensory processing in health and disease. Although some experimental data suggest the posterior insula in rodents can be activated by somatosensory stimuli (Becerra, Chang, Bishop, & Borsook, 2011; Rodgers, et al., 2008), no experimental data to our knowledge has shown that this area is cold-responsive. Indeed, it has been argued that rodents lack critical anatomical pathways for thermo- and pain sensation that are found in humans, suggesting that mechanisms for sensation might be fundamentally different in non-human vertebrates (Craig, 2009b). In cats, neurons in the posterior insula respond to cold stimuli delivered to the tongue (Landgren, 1957), although the number of cold-responsive neurons identified was very small (<5%), suggesting that a modality-specific representation in this area might be sparse. Highly dispersed cells present a challenge for stimulus-specific detection, since a small number of activated cells might be difficult to find and isolate, especially if anatomical landmarks for recording or image registration are not precise.

Here we investigated the cortical representation for cool sensation in the mouse, taking advantage of molecular genetic tools and imaging methodologies to test the hypothesis that the posterior insula is involved in cold sensation. The receptor ion channel TrpM8 is required for thermal sensation in the 15-22°C range, and TrpM8 receptor knock-out mice show no thermal preference in a two-temperature plate assay (Bautista et al., 2007; Colburn et al., 2007; Dhaka et al., 2007; McKemy, Neuhausser, & Julius, 2002). The thermal and chemical sensitivity of this receptor provides complementary methods to activate this specific pathway, and TrpM8 gene knock-outs enabled us to examine responses in the absence of this receptor (Bautista, et al., 2007; Colburn, et al., 2007; Dhaka, et al., 2007).

First, we optimized stimulus parameters for maximizing TrpM8-based neural activation, using expression of the immediate-early gene *c-fos* in the spinal cord to quantitatively compare both cold and menthol stimulation for different somatic locations. Next, using methods adapted from fMRI in humans, we developed a quantitative approach for detecting sparsely activated cells across the brain, using wide-scale *c-fos* immunoreactivity (*fos*-IR) combined with automated cell detection and image registration for across-animal averaging to identify responsive areas. Finally, we compared activation patterns in wild-type animals to those in TrpM8 receptor knock-out mice. Our data suggest that the posterior insula in mice, as in humans, is involved in TrpM8-mediated cool sensation.

Materials and Methods

Experimental Procedures

Animals: Male and female C57BL/6 (Jackson Labs) and homozygous *Trpm8*^{tm1Apat/J} knock-out (Jackson Labs) aged 7-12 weeks were accustomed to handling and isoflurane anesthesia 5 days prior to stimulation. All animal work was performed in accordance

with protocols approved by the Institutional Animal Care and Use Committees at Carnegie Mellon University following the National Institutes of Health regulations.

Stimulation: The animals were removed from their homecage, lightly anaesthetized with isoflurane in a glass jar, removed after ~10 seconds, at which point their right hindpaw or forepaw was immersed in ice-cold water, room temperature 500mM menthol (Sigma) in 70% ethanol solution, or the vehicle solution alone (control). Animals were returned to their home cage following each stimulation episode. This was repeated 5-10 times (due to variations in recovery time), with ~1 minute intervals between stimulation. Because the menthol solution was not washed off the paw at the end of the trial, it is likely that the stimulus persisted for many minutes after the end of the trial.

Immunohistochemistry: Following stimulation, mice were returned to their home cage for 1 hour. They were then sacrificed with CO₂ or isoflurane and transcardially perfused with phosphate buffered saline (PBS) at 4°C followed by 4% paraformaldehyde (PFA) in 0.1M PBS and 15% saturated Picric acid at 4°C. All perfusions were carried out between 60 and 90 minutes following stimulation. Brains and spinal cords were dissected and postfixed in 4% PFA in 0.1M PBS at 4°C overnight, then cryoprotected in 30% sucrose. 50-µm coronal sections were obtained with a freezing microtome. Free floating sections were first washed in PBS 3 x 10 min, PBS-T for 45 min, blocked in normal goat serum for 1hr, incubated in (rabbit) anti-c-fos PC38T (Ab-5; Santa Cruz) diluted in PBS-Triton x-100 (1:5000) for 48 hours. The sections were then washed in PBS-T for 3 x 10 min followed by a 3 hour incubation at room temperature in [Alexa Fluor® 546 goat anti-rabbit](#) (Life Technologies) diluted 1:500 in PBS-T. Sections were then rinsed in PBS-T twice followed by a final rinse in PBS. Sections were mounted on Superfrost slides with vectashield mounting medium with DAPI (Vector Laboratories).

Imaging: Digital images were acquired on an Olympus BX51WI microscope equipped with a Olympus XL Fluor 4x/340 NA 0.28 lens with a Retiga 2000R camera. Exposure times were 500 ms. Spinal cord images were captured in a single image. For coronal brain sections, 2-4 images were acquired for each section which were then stitched together using ImageJ's automated pairwise stitching plugin set to max intensity (available at <http://fiji.sc>).

Quantification of fos-IR expression: For spinal cord images, fos-IR cells were manually counted in the dorsal horn across 4-6 sections per animal, and then these values were averaged across animals. For brain images, the large number of fos-IR cells required the development of automated analysis protocols to cover the entire cerebral cortex (Figure 1). Our protocol consisted of a template matching algorithm common in computer vision, adapted for neuron counting (Brunelli, 2009). Brain sections were selected based on visual comparison to the Nissl stained Allen Brain Atlas images (Figure 1A; <http://brain-map.org/>), in addition to anatomical landmarks, including the relative size of the lateral ventricles and the hippocampus. Post-staining, individual sections were imaged and stitched using intensity-based image registration (Fiji plug-in for ImageJ) into a single image file corresponding to the entire coronal section for analysis (Figure 1B). To automate detection of fos-IR cells in cortex, we first identified representative template cells ($n=4$) that exhibited clear fos-IR signal. Template windows represented fos-IR cells of variable size and intensity from multiple regions of the brain. The entire image ($\sim 1400 \times 1500$ pixels) was then scanned using a sliding box window (7x7 pixels) and the pixel intensities in that region was correlated with the intensities of the template cells. If the correlation (custom Matlab function `normxcorr2`) between the template and the pixel intensities in that region exceeded ~ 0.88 , a cell was counted at

that location. This threshold was set so that the algorithm output would match the number of strongly labeled, visually-identifiable fos-IR cells from inspection of a tissue section (Figure 1B, inset). An example image showing the absolute and mean locations of counted neurons in a menthol-stimulated wildtype animal is shown in Figure 1C and D. Cell counts were then binned in 30x30 pixel windows ($\sim 10 \mu\text{m}^2$) and visualized using a standard heat map (Matlab function heatmap) (Figure 1E,F). Importantly, automated cell counts were not sensitive to image contrast (Figure 1B,E,C,F), so that the same analysis could be used across samples of varying fluorescence intensity. Results from ~ 3 sections spanning 150 microns centered at each of 4 bregma locations (-0.4 mm, -0.8 mm, -1.3 mm, -1.6 mm) were then averaged (Figure 1 G,H). In some cases (<15%), damaged tissue or incompletely stained tissue sections from an animal series were omitted from the analysis, since they could not be properly aligned.

Statistical analysis. For the spinal cord analysis, we counted the number of positively labeled cells in the medial, central and lateral dorsal horn. Counts were averaged across each section (n=4). These average counts were then averaged across animals (n=4 (menthol stimulation) or n=6 (cold stimulation)). For spinal cord samples, different stimulation protocols were compared with a two-sample t-test and adjusted for multiple comparisons using Bonferroni correction.

For analysis of fos-IR cells in brain sections, FIJI was used to draw ROIs for a given brain region. These template ROIs were applied to individual brain sections for automated counting using MatLab (custom function normxcorr2_trained_heatmap.m). ROI templates were overlaid upon the same aligned image stack used to generate the averaged heatmap cell counts show in Figure 6, and alignments for individual sections could vary slightly. Since the number of animals in each condition varied, differences in these average cell counts across conditions was statistically evaluated using one-way

ANOVA. When ANOVA indicated a significant group average difference, a Bonferroni correction for multiple comparisons within a condition was employed.

Results

Menthol strongly activates neurons in the spinal cord

Cool sensation is thought to be initiated through the activation of TrpM8-expressing neurons with free nerve endings distributed in a patchy manner across the skin (Hensel, 1982; Takashima et al., 2007). Some studies have suggested that the density of TrpM8-expressing fibers is non-uniform, with a higher density of “cold spots” in some areas (Strughold & Porz, 1931), although this has not been systematically evaluated across the entire body surface. Using expression of the activity-dependent transcription factor c-fos in the spinal cord, the site of the first synapse from TrpM8-expressing DRG neurons to the central nervous system (CNS), we compared levels of activation within the dorsal horn of the spinal cord using either forepaw or hindpaw cold- or menthol stimulation in anaesthetized animals. Spinal cord tissue was dissected out and subject to c-fos immunohistochemistry and imaging.

In all cases, stimulation was associated with an increase in fos-IR cells in the ipsilateral versus the contralateral portion of the spinal cord. Fos-IR cells were concentrated in superficial lamina, the site of pain and temperature responsive second-order neurons (Figure 2). The majority of fos-IR cells lay at the medial edge of the dorsal horn, consistent with the medial-to-lateral mapping of distal-to-proximal cutaneous afferents in the dorsal horn (Brown & Fuchs, 1975; Koerber, 1980).

Cold and menthol stimulation yielded quantitatively different results, with menthol inducing significantly greater number of activated cells (Figure 2). In thoracic regions of

the spinal cord, cold stimulation of the forepaw significantly increased the number of fos-IR cells in lamina 1-2 compared to the unstimulated, contralateral side (cold 9.75 ± 2.4 cells vs unstimulated side 2.37 ± 0.5 cells; $n=4$ animals per condition; Figure 2D). Cold-induced levels of activation in lumbar regions of the spinal cord were similar with hindpaw stimulation (cold 10.5 ± 4.1 cells vs unstimulated side 2.56 ± 1.4 cells; $n=4$ animals per condition).

Menthol stimulation yielded robust and highly significant response compared to the contralateral spinal cord for both the forepaw (menthol 37 ± 2.23 cells vs unstimulated side 8.6 ± 0.84 cells; $n=6$ animals per condition) and the hindpaw (menthol 75.1 ± 13.8 cells versus unstimulated side 17.3 ± 3.5 cells; $n=6$ animals per condition). Overall, the number of fos-IR cells was significantly greater for menthol application to the hindpaw than the forepaw.

For both fore- and hindpaw stimulation, menthol induced a significantly larger response compared to cold. The total number of fos-IR cells was greatest following menthol stimulation of the hindpaw, with >7-fold more cells labeled than with hindpaw application of a cold stimulus.

High-throughput, semiautomated analysis of menthol-induced fos-IR

Because menthol stimulation to the hindpaw induced the most robust fos-IR signal in the spinal cord, this stimulus was selected to drive activity-dependent gene expression to identify brain areas responsive to TrpM8 activation. Animals were subjected to menthol stimulation as described above, and approximately 2 mm of tissue centered around somatosensory neocortical areas from the stimulated-side hemisphere was sectioned at 50 μm thickness and stained for fos-IR

Automated analysis enabled us to quantitatively survey fos-IR cells in all sections across a broad region of the brain for an individual animal. Unlike other somatosensory

stimuli such as single-whisker stimulation that generate a robust, dense area of fos-IR cells throughout a cortical column (see for example (Barth, Gerkin, & Dean, 2004)), we did not observe regional clustering of fos-IR cells after menthol stimulation in any neocortical area. However, this method was sensitive enough to highlight some specific brain areas for us to focus on for further analysis. Specifically, we selected tissue sections that represented primary somatosensory cortex (bregma -0.3 to -1.2), S2, and the posterior insula (bregma -0.4 to -1.3) for averaging within and across animals to enhance stimulus-related signal. This process was carried out for both menthol- and vehicle-stimulated animals.

Whole-cell recordings in superficial layers of S1 have shown that cool stimulation delivered to the forepaw can depolarize neurons and lead to spiking of some cells (Milenkovic, et al., 2014). Thus, we expected that we might observe menthol-evoked fos-IR in the S1 area corresponding to the hindpaw. Indeed, a low level of menthol-activated fos-IR was apparent in both superficial and deep layers of the S1 hindpaw region at bregma -0.8 (Figure 3A,B). A more prominent signal was observed in regions lateral to S1, in a dispersed subset of cells in a region surrounding the posterior insula and S2, extending for several hundred microns, could be observed in menthol-stimulation animals (Figure 3C; bregma -1.3 and posterior sections). Fos-IR signal extending across the posterior piriform was also apparent after menthol stimulation.

The sparse distribution of activated cells was difficult to observe by visual inspection from individual sections, but was apparent when adjacent sections were aligned and averaged from the same animal and then across animals (see Figure 1 for methods; Figure 3). Fos-IR signal was low in both vehicle-stimulated (Figure 3E-H) and unstimulated control animals (not shown).

We also examined the pattern of activation induced by menthol stimulation to the forepaw, which was qualitatively lower than that induced by hindpaw stimulation (data

not shown). Because the forepaw-induced signal was low, and because fos-IR signal was visualized by average adjacent sections, covering ~150 μm of brain tissue, it was difficult to determine whether the menthol-induced response was somatotopic, with forepaw activation anterior to hindpaw areas. Because forepaw-evoked c-fos expression was weaker than hindpaw-evoked responses, both in the spinal cord and in the brain, all subsequent experiments were carried out using hindpaw stimulation.

Menthol activates subcortical brain areas

Other notable areas robustly activated by menthol exposure to the hindpaw were the hypothalamus, particularly the anterior hypothalamic nucleus, the medial thalamic nuclei, the lateral and basolateral amygdala, and the posterior piriform cortex (Figure 3A-D). The fact that we observed reliable hypothalamic activation is broadly consistent with thermal regulatory responses associated with TrpM8 activation (Nakamura & Morrison, 2007). However, the relatively small size of these regions (especially in the hypothalamus, nuclei can be $<100 \mu\text{m}$) and intra-subject variability in image registration for signal averaging preclude drawing precise conclusions about subnuclei within the hypothalamus and thalamus.

TrpM8 knock-out animals lack menthol-induced activation

An advantage of studying cool sensation is that this response is mediated fully via expression of the TrpM8 receptor, since mice lacking TrpM8 cannot detect temperatures in the 14-24°C range (Bautista, et al., 2007; Colburn, et al., 2007; Dhaka, et al., 2007; Milenkovic, et al., 2014). This provides an approach to investigate the TrpM8-specificity of the menthol-evoked signal observed in the posterior insula and S2. TrpM8 knock-out mice (Takashima, Ma, & McKemy, 2010) were subject to hindpaw menthol exposure and processed for fos-IR. We predicted that if the fos-IR signal

detected was due to activation of the TrpM8 receptor, animals exposed to menthol but lacking this receptor would no longer show elevated fos-IR signal in identified brain areas.

Notably, menthol-induced fos-IR signal was negligible in TrpM8 knock-out mice, assessed using the same automated analysis and image averaging described above (Figure 4). Both the putative posterior insula and S2, as well as hypothalamic and amygdala regions, showed no specific fos-IR induction, and were similar to vehicle-stimulated animals or unstimulated controls. These data are consistent with the hypothesis that TrpM8-activity induced by cutaneous menthol application is associated with neural activity in the brain areas identified in Figure 3.

Piriform cortex: olfactory locus for menthol-related responses?

Menthol is one of the active ingredients in peppermint, a volatile compound originally isolated from plants. Peppermint exposure elicits a direct olfactory response in the olfactory epithelium and olfactory bulb as well as the piriform cortex (Shakhawat et al., 2014), though this olfactory region is typically localized to the anterior piriform area (Wilson & Sullivan, 2011). Thus, the piriform activation we observed with menthol application to the hindpaw might be attributed to a parallel olfactory response mediated through menthol-activated G-protein coupled receptors (GPCRs) in the olfactory epithelium. Alternatively, fos-IR in the posterior piriform might be mediated through afferents in the skin or respiratory mucosa, which is densely innervated by TrpM8-expressing nerve endings (S. C. Liu et al., 2015). Indeed, volatile menthol is commonly used as a decongestant and cough suppressant due to its influence on TrpM8 afferents in the respiratory mucosa. To evaluate whether the piriform activation we observed was through TrpM8 activation, or coincident menthol activation of olfactory receptors GPCRs,

we examined fos-IR after exposure to volatile menthol in both wild-type and TRPM8 knock-out mice.

Animals were exposed to menthol via exposure to a saturated paper tissue mounted above the holding cage for 2 hrs prior to sacrifice. Automated analysis of brain fos-IR with volatile menthol exposure revealed strong signal at bregma -1.3 and more posterior regions, with somewhat reduced activation in hypothalamic areas (Figure 5). In addition, the anterior piriform cortex appeared to be more strongly labeled than posterior piriform areas (Figure 5). Thus, volatile menthol was sufficient to activate fos-IR in similar brain areas compared to topical application to the hindpaw.

Interestingly, this pattern of menthol-related activation in piriform cortex was absent in TrpM8 knock-out mice (Figure 5), suggesting that piriform fos-IR in wildtype menthol-exposed animals is mediated by TrpM8-expressing neurons, not via menthol-specific receptors expressed by sensory neurons in the olfactory epithelium.

Quantitative comparisons of menthol-evoked responses

For quantitative and statistical comparison of menthol-evoked fos-IR across specified brain areas, cell counts for each region of interest were averaged within animal and then across animals (Figure 6). The area of the selected region varied across target, such that the hypothalamus was not the same area as S2, for example. Thus, the absolute number of cells per region could vary, and cell counts across different regions are not directly comparable. Statistical comparison were carried out within an ROI, using a one-way ANOVA.

Overall, menthol treatment to the hindpaw induced a robust response in the hypothalamus and selected areas of the neocortex, and in every case, this response was greater in wildtype animals compared to TrpM8 knock-out mice (Figure 6). In the hypothalamus, the wildtype menthol-stimulated mice showed the largest number of fos-

IR compared to any other condition. In S1 hindpaw, wildtype menthol-treated animals again exhibited significantly higher fos-IR cells than in either the TrpM8 knock-out or wildtype volatile menthol-treated animals, but not in comparison to the wildtype vehicle-treated animals. In S2, the number of fos-IR cells was significantly higher in the wildtype menthol-stimulated mice than in any other condition. In insular cortex, the number of counted cells in wildtype menthol-stimulated mice was significantly higher than the wildtype vehicle and knock-out animals but not significantly different from the volatile menthol-stimulated mice. In piriform cortex, the only detected difference was between wildtype menthol-stimulated mice and TrpM8 knock-out mice.

Discussion

Here we take advantage of a discrete modality of cutaneous thermal information, cold sensation mediated by the TrpM8 receptor, to investigate the neocortical representation of cold. We present data showing that TrpM8 receptor activation can drive immediate-early gene expression in the mouse CNS. Initially we optimized stimulus presentation using spinal cord expression of c-fos to determine that menthol application to the hindpaw elicited the most robust response. We next developed methods for automated, brain-scale analysis of stimulus-evoked c-fos expression, and applied these methods to identify cortical regions that were activated by menthol stimulation. In addition to weak activation in primary somatosensory cortex, we found evoked c-fos expression in more posterior somatosensory-related areas that correspond to S2 and the posterior insula. Menthol-evoked fos-IR in these areas was absent in TrpM8 knock-out mice, indicating that this signal was related to peripheral receptor activation. Our data are consistent with the presence of additional somatosensory maps in rodents outside of S1 that may be specialized for the processing of other cutaneous inputs, similar to areas identified in cats, monkeys, and humans.

Rodent correlates of the posterior insula

In humans, experimental evidence implicates primary somatosensory cortex (S1), S2, as well as insular cortex in the processing of thermal information (Baumgartner, et al., 2010; Bingel et al., 2004; Brooks, et al., 2005; Craig, et al., 2000; Duerden & Albanese, 2013; Ferretti et al., 2003; Frot & Mauguiere, 2003; Greenspan, et al., 2008; Iannetti, Zambreanu, Cruccu, & Tracey, 2005; Kanda et al., 2000; Liang, Mouraux, & Iannetti, 2011; Mancini, Haggard, Iannetti, Longo, & Sereno, 2012; Ploner, Schmitz, Freund, & Schnitzler, 1999; Rios, Treede, Lee, & Lenz, 1999; Valentini et al., 2012).

Despite strong evidence that S1 is activated by thermal stimuli, some lesion and microstimulation studies suggest a non-essential role of this area in temperature sensation. For example, parietal lobe (S1) lesions are not associated with a loss of temperature sensation (Biernacki, 1955; Holmes, 1927; Kleist, 1934), and early microstimulation studies in human parietal cortex rarely elicited thermal percepts (Penfield & Boldry, 1937). In contrast, lesions in the posterior insula and S2 have been associated with loss of pinprick pain and thermal sensation (Birklein, et al., 2005; Davis, et al., 2004; Greenspan, Lee, & Lenz, 1999; Greenspan & Winfield, 1992).

Several important findings support the hypothesis that the insula may be an independent primary somatosensory area specialized for cool temperature perception. First, human imaging studies identify the posterior insula as a cold-responsive area (Craig, et al., 2000), and microstimulation studies in human posterior insula are sufficient to elicit cold and also pain sensation (Ostrowsky et al., 2002). Second, a number of early 20th century studies as well as some contemporary studies have associated insular lesions with abnormal pain and temperature sensation (Biernacki, 1955; Birklein, et al., 2005; Holmes, 1927; Kleist, 1934). In at least one case study insular lesions were associated with a somatotopically-restricted elimination of pinprick pain and cold sensation without loss of more complex tactile senses such as tactile object recognition

or two point discrimination (Birklein, et al., 2005). The complete loss of sensation indicates that the posterior insula may not merely carry a copy of nociceptive and thermal information from S1, but may be a direct thalamic target for this stream of peripheral input.

Rodents enable the use of superior tools and experimental methodologies to investigate the transmission of thermal information in the CNS in health and disease. However, it has been argued that anatomical pathways that mediate these responses in humans are absent in rats and mice (Craig, 2009b). In particular, rodent correlates of the dorsal posterior insula, or an equivalent to the projecting thalamic region in primates (the ventromedial nucleus, VMPO) have been disputed, and without these structures thermal (and nociceptive) awareness may be limited (Craig, 2009b). However, experimental evidence from the rat has shown an S1-independent somatotopic-evoked response in the insula (Rodgers, et al., 2008), and neurons in the POT (triangular posterior nucleus, a thalamic nucleus that may be equivalent to VMPO; (Jaenig, 2006)) respond to nociceptive and thermal stimuli and have direct axonal projections to the insula and S2 (Gauriau & Bernard, 2004). Thus, it is plausible that cold sensation may map to a posterior and lateral location that corresponds to the insula in rodents as it does in primates.

It has not been established whether thermal and nociceptive inputs arrive simultaneously at these different brain regions, or are processed in series, with a primary representation in S1 (Bingel, et al., 2004; Ferretti, et al., 2003; Kanda, et al., 2000; Liang, et al., 2011; Ploner, et al., 1999). Our data do not directly evaluate this. Because the insula is also involved in the emotional/affective arm of the pain matrix, activation in this region may be secondary to early somatosensory responses that we did not detect by fos-IR. Indeed, pain-related neocortical activation has been observed in anterior cingulate and orbitofrontal areas (Bushnell et al., 1999; Craig, et al., 2000; D.R.

Kenshalo & Willis, 1991; Landgren, 1957; Oshiro, Quevedo, McHaffie, Kraft, & Coghill, 2007; Ploner, Gross, Timmermann, & Schnitzler, 2002; Treede, Kenshalo, Gracely, & Jones, 1999), and the insula is also involved in the affective/emotional aspects of pain sensation (Craig, 2009a; Nagai, Kishi, & Kato, 2007; Nieuwenhuys, 2012; Shackman et al., 2011).

Cold-evoked fos-IR activation was weak in both spinal cord and neocortex

Surprisingly, we did not observe strong spinal cord or brain activation elicited by cold (ice water) stimulation. Cold stimulation elicited weak fos-IR in the spinal cord and no discernable fos-IR cortical signal (data not shown). Ice water may stimulate other cold receptors besides TrpM8, as it extends into the noxious cold range, and prolonged exposure to thermal stimuli may be associated with receptor desensitization. Extreme cold stimuli may also activated additional sensory pathways, specifically those associated with cold pain. However, we note that the distinction between innocuous and noxious cold (cool versus cold) has been difficult to define in animals, and in humans, noxious cold thresholds span wide temperature range (0-28°C) across individuals (Erpelding, Moayed, & Davis, 2012). Experimental evidence in humans suggests that both noxious and innocuous cold sensation likely to map to similar cortical locations (Craig, et al., 2000); we hypothesize that this is conserved in mice. It is also notable that hindpaw activation was much more effective at driving fos-IR in both the spinal cord and the brain. These data suggest that the distribution of TrpM8 receptors may be concentrated in the lower extremities. Our findings suggest that perceptual sensitivity to cool stimuli may be most pronounced when these stimuli are delivered to the hindpaw.

These findings complement results from Milenkovic et al., where whole-cell patch clamp recordings in awake mice demonstrated that neurons in superficial layers of S1 can depolarize in response to forepaw cooling. Importantly, pharmacological blockade of this region abolished cool detection during a Peltier-driven choice assay (Milenkovic,

et al., 2014). However, the magnitude of the reported depolarization for S1 neurons in response to cooling may not have been sufficient to drive fos-IR, which typically requires elevations in firing activity (Fields, Eshete, Stevens, & Itoh, 1997; Schoenenberger, Gerosa, & Oertner, 2009). Although behavioral report of cool stimulation required S1 in this study, it remains unclear whether this reflects S1 as the only neocortical region sensory region required for cool perception. Alternatively, S1 activity might be evoked in parallel with S2 and insular activation, providing a fine-grained topographic map that enables stimulus localization. *In vivo* recordings from neurons in S2 and posterior insula will help determine whether fos-IR in these regions can be linked to rapid TrpM8-associated activation of neural firing.

Conclusions

It has long been appreciated that thermal and nociception are anatomically linked, both in the spinal cord and the brain. Determining how temperature is represented in the neocortex will enable investigations into how broad-scale somatosensory maps can be changed by experience. Cool sensation is a particularly advantageous modality to employ for cortical mapping studies, since it is not accompanied by many of the affective components of nociceptor activation.

TrpM8 was an ideal receptor subtype to investigate, since it is the only receptor that can be activated within a defined (cool) thermal range, in contrast to the redundant sensitivity of receptors for the warm-hot range (Jordt, McKemy, & Julius, 2003). The existence of highly-specific chemical ligands that can activate TrpM8 also provides an additional way to selectively activate this receptor, and menthol stimulation in TrpM8 knock-out animals enabled a strict test of the role of cutaneous activation in driving neocortical responses. Understanding the basic anatomical and electrophysiological properties of brain areas involved in thermal and nociceptive processing will be a critical

step in understanding how these circuits can be altered by experience and disease, and ultimately in developing better treatments for pain disorders.

Acknowledgements

All authors had full access to all the data in the study and participated in data acquisition and analysis. Specific roles were as follows: Study concept and design: PB, SN, YT, AB; Acquisition of data: PB, KC, EP, VM; Analysis and interpretation of data: SN, PB, YT, KC, VM, EP, AB; Drafting of the manuscript: PB, AB; Statistical analysis: PB; Obtained funding: AB; Critical revision of the manuscript for important intellectual content: PB, SN, AB. All authors read and contributed to the writing of the manuscript.

Accepted

References

- Baier, B., zu Eulenburg, P., Geber, C., Rohde, F., Rolke, R., Maihofner, C., . . . Dieterich, M. (2014). Insula and sensory insular cortex and somatosensory control in patients with insular stroke. [Research Support, Non-U.S. Gov't]. *European journal of pain*, *18*(10), 1385-1393. doi: 10.1002/j.1532-2149.2014.501.x
- Barth, A. L., Gerkin, R. C., & Dean, K. L. (2004). Alteration of neuronal firing properties after in vivo experience in a FosGFP transgenic mouse. *J Neurosci*, *24*(29), 6466-6475.
- Baumgartner, U., Iannetti, G. D., Zambreanu, L., Stoeter, P., Treede, R. D., & Tracey, I. (2010). Multiple somatotopic representations of heat and mechanical pain in the operculo-insular cortex: a high-resolution fMRI study. [Research Support, Non-U.S. Gov't]. *Journal of neurophysiology*, *104*(5), 2863-2872. doi: 10.1152/jn.00253.2010
- Bautista, D. M., Siemens, J., Glazer, J. M., Tsuruda, P. R., Basbaum, A. I., Stucky, C. L., . . . Julius, D. (2007). The menthol receptor TRPM8 is the principal detector of environmental cold. *Nature*.
- Becerra, L., Chang, P. C., Bishop, J., & Borsook, D. (2011). CNS activation maps in awake rats exposed to thermal stimuli to the dorsum of the hindpaw. [Research Support, N.I.H., Extramural Research Support, Non-U.S. Gov't]. *NeuroImage*, *54*(2), 1355-1366. doi: 10.1016/j.neuroimage.2010.08.056
- Biemond, A. (1955). The conduction of pain above the level of the thalamus opticus. *AMA Archives of Neurology and Psychiatry*, 231-244.
- Bingel, U., Lorenz, J., Glauche, V., Knab, R., Glascher, J., Weiller, C., & Buchel, C. (2004). Somatotopic organization of human somatosensory cortices for pain: a single trial fMRI study. [Research Support, Non-U.S. Gov't]. *NeuroImage*, *23*(1), 224-232. doi: 10.1016/j.neuroimage.2004.05.021
- Birklein, F., Rolke, R., & Muller-Forell, W. (2005). Isolated insular infarction eliminates contralateral cold, cold pain, and pinprick perception. *Neurology*, *65*(9), 1381.
- Brooks, J. C., Zambreanu, L., Godinez, A., Craig, A. D., & Tracey, I. (2005). Somatotopic organisation of the human insula to painful heat studied with high resolution functional imaging. [Clinical Trial Research Support, N.I.H., Extramural Research Support, Non-U.S. Gov't Research Support, U.S. Gov't, P.H.S.]. *NeuroImage*, *27*(1), 201-209. doi: 10.1016/j.neuroimage.2005.03.041
- Brown, P. B., & Fuchs, J. L. (1975). Somatotopic representation of hindlimb skin in cat dorsal horn. [Research Support, U.S. Gov't, P.H.S.]. *Journal of neurophysiology*, *38*(1), 1-9.
- Bushnell, M. C., Duncan, G. H., Hofbauer, R. K., Ha, B., Chen, J. I., & Carrier, B. (1999). Pain perception: is there a role for primary somatosensory cortex? *Proc Natl Acad Sci U S A*, *96*(14), 7705-7709.
- Casey, K. L., Minoshima, S., Morrow, T. J., & Koeppe, R. A. (1996). Comparison of human cerebral activation pattern during cutaneous warmth, heat pain, and deep cold pain. [Clinical Trial Comparative Study Controlled Clinical Trial Research Support, U.S. Gov't, Non-P.H.S.]. *Journal of neurophysiology*, *76*(1), 571-581.

- Colburn, R. W., Lubin, M. L., Stone, D. J., Jr., Wang, Y., Lawrence, D., D'Andrea, M. R., . . . Qin, N. (2007). Attenuated cold sensitivity in TRPM8 null mice. *Neuron*, *54*(3), 379-386.
- Craig, A. D. (2003). Pain mechanisms: labeled lines versus convergence in central processing. *Annu Rev Neurosci*, *26*, 1-30.
- Craig, A. D. (2009a). How do you feel--now? The anterior insula and human awareness. *Nat Rev Neurosci*, *10*(1), 59-70.
- Craig, A. D. (2009b). A rat is not a monkey is not a human: comment on Mogil (Nature Rev. Neurosci. *10*, 283-294 (2009)). *Nat Rev Neurosci*, *10*(6), 466.
- Craig, A. D., Chen, K., Bandy, D., & Reiman, E. M. (2000). Thermosensory activation of insular cortex. *Nat Neurosci*, *3*(2), 184-190.
- Davis, K. D., Kwan, C. L., Crawley, A. P., & Mikulis, D. J. (1998). Functional MRI study of thalamic and cortical activations evoked by cutaneous heat, cold, and tactile stimuli. *J Neurophysiol*, *80*(3), 1533-1546.
- Davis, K. D., Pope, G. E., Crawley, A. P., & Mikulis, D. J. (2004). Perceptual illusion of "paradoxical heat" engages the insular cortex. [Research Support, Non-U.S. Gov't]. *Journal of neurophysiology*, *92*(2), 1248-1251. doi: 10.1152/jn.00084.2004
- Dhaka, A., Murray, A. N., Mathur, J., Earley, T. J., Petrus, M. J., & Patapoutian, A. (2007). TRPM8 is required for cold sensation in mice. *Neuron*, *54*(3), 371-378.
- Duerden, E. G., & Albanese, M. C. (2013). Localization of pain-related brain activation: a meta-analysis of neuroimaging data. [Meta-Analysis Research Support, Non-U.S. Gov't]. *Human brain mapping*, *34*(1), 109-149. doi: 10.1002/hbm.21416
- Egan, G. F., Johnson, J., Farrell, M., McAllen, R., Zamarripa, F., McKinley, M. J., . . . Fox, P. T. (2005). Cortical, thalamic, and hypothalamic responses to cooling and warming the skin in awake humans: a positron-emission tomography study. [Research Support, Non-U.S. Gov't Research Support, U.S. Gov't, P.H.S.]. *Proceedings of the National Academy of Sciences of the United States of America*, *102*(14), 5262-5267. doi: 10.1073/pnas.0409753102
- Erpelding, N., Moayed, M., & Davis, K. D. (2012). Cortical thickness correlates of pain and temperature sensitivity. [Research Support, Non-U.S. Gov't]. *Pain*, *153*(8), 1602-1609. doi: 10.1016/j.pain.2012.03.012
- Ferretti, A., Babiloni, C., Gratta, C. D., Caulo, M., Tartaro, A., Bonomo, L., . . . Romani, G. L. (2003). Functional topography of the secondary somatosensory cortex for nonpainful and painful stimuli: an fMRI study. [Clinical Trial Research Support, Non-U.S. Gov't]. *NeuroImage*, *20*(3), 1625-1638.
- Fields, R. D., Eshete, F., Stevens, B., & Itoh, K. (1997). Action potential-dependent regulation of gene expression: temporal specificity in ca^{2+} , cAMP-responsive element binding proteins, and mitogen-activated protein kinase signaling. *The Journal of neuroscience : the official journal of the Society for Neuroscience*, *17*(19), 7252-7266.
- Frot, M., & Mauguiere, F. (2003). Dual representation of pain in the operculo-insular cortex in humans. *Brain : a journal of neurology*, *126*(Pt 2), 438-450.
- Gauriau, C., & Bernard, J. F. (2004). Posterior triangular thalamic neurons convey nociceptive messages to the secondary somatosensory and insular cortices in the rat. *J Neurosci*, *24*(3), 752-761. doi: 10.1523/JNEUROSCI.3272-03.2004 24/3/752 [pii]
- Greenspan, J. D., Lee, R. R., & Lenz, F. A. (1999). Pain sensitivity alterations as a function of lesion location in the parasyllian cortex. [Research Support, U.S. Gov't, P.H.S.]. *Pain*, *81*(3), 273-282.

- Greenspan, J. D., Ohara, S., Franaszczuk, P., Veldhuijzen, D. S., & Lenz, F. A. (2008). Cold stimuli evoke potentials that can be recorded directly from parasyllian cortex in humans. *J Neurophysiol*, *100*(4), 2282-2286.
- Greenspan, J. D., & Winfield, J. A. (1992). Reversible pain and tactile deficits associated with a cerebral tumor compressing the posterior insula and parietal operculum. [Case Reports Research Support, Non-U.S. Gov't]. *Pain*, *50*(1), 29-39.
- Hensel, H. (1982). *Thermal sensations and thermoreceptors in man*. Springfield, Illinois: Charles C. Thomas.
- Holmes, G. (1927). Disorders of sensation produced by cortical lesions. *Brain*, *50*, 413-427.
- Iannetti, G. D., Zambreanu, L., Cruccu, G., & Tracey, I. (2005). Operculoinsular cortex encodes pain intensity at the earliest stages of cortical processing as indicated by amplitude of laser-evoked potentials in humans. [Research Support, Non-U.S. Gov't]. *Neuroscience*, *131*(1), 199-208. doi: 10.1016/j.neuroscience.2004.10.035
- Jaenig, Wilfred. (2006). *The integrated action of the autonomic nervous system*. Cambridge: Cambridge University Press.
- Jordt, S. E., McKemy, D. D., & Julius, D. (2003). Lessons from peppers and peppermint: the molecular logic of thermosensation. *Curr Opin Neurobiol*, *13*(4), 487-492.
- Kaas, J. H., & Collins, C. E. (2003). The organization of somatosensory cortex in anthropoid primates. [Review]. *Advances in neurology*, *93*, 57-67.
- Kanda, M., Nagamine, T., Ikeda, A., Ohara, S., Kunieda, T., Fujiwara, N., . . . Shibasaki, H. (2000). Primary somatosensory cortex is actively involved in pain processing in human. [Clinical Trial Controlled Clinical Trial Research Support, Non-U.S. Gov't]. *Brain research*, *853*(2), 282-289.
- Kenshalo, D. R., Iwata, K., Sholas, M., & Thomas, D. A. (2000). Response properties and organization of nociceptive neurons in area 1 of monkey primary somatosensory cortex. *J Neurophysiol*, *84*(2), 719-729.
- Kenshalo, D.R., & Willis, W.D. Jr. (1991). *The role of the cerebral cortex in pain*. Kleist, K. (1934). *Gehirnpathologie*. Leipzig: J.A. Barth.
- Koerber, H. R. (1980). Somatotopic organization of cat brachial spinal cord. [Research Support, Non-U.S. Gov't Research Support, U.S. Gov't, P.H.S.]. *Experimental neurology*, *69*(3), 481-492.
- Krubitzer, L. A., & Calford, M. B. (1992). Five topographically organized fields in the somatosensory cortex of the flying fox: microelectrode maps, myeloarchitecture, and cortical modules. [Research Support, Non-U.S. Gov't]. *The Journal of comparative neurology*, *317*(1), 1-30. doi: 10.1002/cne.903170102
- Landgren, S. (1957). Cortical reception of cold impulses from the tongue of the cat. *Acta Physiol Scand*, *40*(2-3), 202-209.
- Liang, M., Mouraux, A., & Iannetti, G. D. (2011). Parallel processing of nociceptive and non-nociceptive somatosensory information in the human primary and secondary somatosensory cortices: evidence from dynamic causal modeling of functional magnetic resonance imaging data. [Research Support, Non-U.S. Gov't]. *The Journal of neuroscience : the official journal of the Society for Neuroscience*, *31*(24), 8976-8985. doi: 10.1523/JNEUROSCI.6207-10.2011
- Liu, S. C., Lu, H. H., Cheng, L. H., Chu, Y. H., Lee, F. P., Wu, C. C., & Wang, H. W. (2015). Identification of the cold receptor TRPM8 in the nasal mucosa. [Research Support, Non-U.S. Gov't]. *American journal of rhinology & allergy*, *29*(4), e112-116. doi: 10.2500/ajra.2015.29.4202
- Liu, Y., & Ma, Q. (2011). Generation of somatic sensory neuron diversity and implications on sensory coding. [Research Support, N.I.H., Extramural Review]. *Current opinion in neurobiology*, *21*(1), 52-60. doi: 10.1016/j.conb.2010.09.003

- Mancini, F., Haggard, P., Iannetti, G. D., Longo, M. R., & Sereno, M. I. (2012). Fine-grained nociceptive maps in primary somatosensory cortex. [Research Support, N.I.H., Extramural Research Support, Non-U.S. Gov't]. *The Journal of neuroscience : the official journal of the Society for Neuroscience*, *32*(48), 17155-17162. doi: 10.1523/JNEUROSCI.3059-12.2012
- Mazzola, L., Faillenot, I., Barral, F. G., Mauguiere, F., & Peyron, R. (2012). Spatial segregation of somato-sensory and pain activations in the human operculo-insular cortex. *NeuroImage*, *60*(1), 409-418. doi: 10.1016/j.neuroimage.2011.12.072
- McKemy, D. D., Neuhausser, W. M., & Julius, D. (2002). Identification of a cold receptor reveals a general role for TRP channels in thermosensation. *Nature*, *416*(6876), 52-58.
- Milenkovic, N., Zhao, W. J., Walcher, J., Albert, T., Siemens, J., Lewin, G. R., & Poulet, J. F. (2014). A somatosensory circuit for cooling perception in mice. [Research Support, Non-U.S. Gov't]. *Nature neuroscience*, *17*(11), 1560-1566. doi: 10.1038/nn.3828
- Nagai, M., Kishi, K., & Kato, S. (2007). Insular cortex and neuropsychiatric disorders: a review of recent literature. *Eur Psychiatry*, *22*(6), 387-394.
- Nakamura, K., & Morrison, S. F. (2007). Central efferent pathways mediating skin cooling-evoked sympathetic thermogenesis in brown adipose tissue. [Research Support, N.I.H., Extramural Research Support, Non-U.S. Gov't]. *American journal of physiology. Regulatory, integrative and comparative physiology*, *292*(1), R127-136. doi: 10.1152/ajpregu.00427.2006
- Nieuwenhuys, R. (2012). The insular cortex: a review. [Review]. *Progress in brain research*, *195*, 123-163. doi: 10.1016/B978-0-444-53860-4.00007-6
- Oshiro, Y., Quevedo, A. S., McHaffie, J. G., Kraft, R. A., & Coghill, R. C. (2007). Brain mechanisms supporting spatial discrimination of pain. *J Neurosci*, *27*(13), 3388-3394.
- Ostrowsky, K., Magnin, M., Ryvlin, P., Isnard, J., Guenot, M., & Mauguiere, F. (2002). Representation of pain and somatic sensation in the human insula: a study of responses to direct electrical cortical stimulation. *Cereb Cortex*, *12*(4), 376-385.
- Penfield, W., & Boldry, E. (1937). Somatic, motor, and sensory representation in the cerebral cortex of man as studied by electrical stimulation. *Brain*, *60*, 389-443.
- Ploner, M., Gross, J., Timmermann, L., & Schnitzler, A. (2002). Cortical representation of first and second pain sensation in humans. *Proc Natl Acad Sci U S A*, *99*(19), 12444-12448.
- Ploner, M., Schmitz, F., Freund, H. J., & Schnitzler, A. (1999). Parallel activation of primary and secondary somatosensory cortices in human pain processing. *J Neurophysiol*, *81*(6), 3100-3104.
- Rios, M., Treede, R., Lee, J., & Lenz, F. A. (1999). Direct Evidence of Nociceptive Input to Human Anterior Cingulate Gyrus and Parasyllian Cortex. *Current review of pain*, *3*(4), 256-264.
- Rodgers, K. M., Benison, A. M., Klein, A., & Barth, D. S. (2008). Auditory, somatosensory, and multisensory insular cortex in the rat. *Cereb Cortex*, *18*(12), 2941-2951. doi: 10.1093/cercor/bhn054bhn054 [pii]
- Schoenenberger, P., Gerosa, D., & Oertner, T. G. (2009). Temporal control of immediate early gene induction by light. [Research Support, Non-U.S. Gov't]. *PloS one*, *4*(12), e8185. doi: 10.1371/journal.pone.0008185

- Shackman, A. J., Salomons, T. V., Slagter, H. A., Fox, A. S., Winter, J. J., & Davidson, R. J. (2011). The integration of negative affect, pain and cognitive control in the cingulate cortex. *Nat Rev Neurosci*, *12*(3), 154-167.
- Shakhawat, A. M., Gheidi, A., Hou, Q., Dhillon, S. K., Marrone, D. F., Harley, C. W., & Yuan, Q. (2014). Visualizing the engram: learning stabilizes odor representations in the olfactory network. [Research Support, Non-U.S. Gov't]. *The Journal of neuroscience : the official journal of the Society for Neuroscience*, *34*(46), 15394-15401. doi: 10.1523/JNEUROSCI.3396-14.2014
- Stephani, C., Fernandez-Baca Vaca, G., Maciunas, R., Koubeissi, M., & Luders, H. O. (2011). Functional neuroanatomy of the insular lobe. [Research Support, Non-U.S. Gov't]. *Brain structure & function*, *216*(2), 137-149. doi: 10.1007/s00429-010-0296-3
- Strughold, H., & Porz, R. (1931). Der dichte der Kahlpuncte auf der Haut der menschlichen Korper *Zoologische Biology*, *91*, 563-571.
- Takashima, Y., Daniels, R. L., Knowlton, W., Teng, J., Liman, E. R., & McKemy, D. D. (2007). Diversity in the neural circuitry of cold sensing revealed by genetic axonal labeling of transient receptor potential melastatin 8 neurons. *J Neurosci*, *27*(51), 14147-14157.
- Takashima, Y., Ma, L., & McKemy, D. D. (2010). The development of peripheral cold neural circuits based on TRPM8 expression. [In Vitro Research Support, N.I.H., Extramural]. *Neuroscience*, *169*(2), 828-842. doi: 10.1016/j.neuroscience.2010.05.039
- Treede, R. D., Kenshalo, D. R., Gracely, R. H., & Jones, A. K. (1999). The cortical representation of pain. *Pain*, *79*(2-3), 105-111.
- Valentini, E., Hu, L., Chakrabarti, B., Hu, Y., Aglioti, S. M., & Iannetti, G. D. (2012). The primary somatosensory cortex largely contributes to the early part of the cortical response elicited by nociceptive stimuli. [Research Support, Non-U.S. Gov't]. *NeuroImage*, *59*(2), 1571-1581. doi: 10.1016/j.neuroimage.2011.08.069
- Wilson, D. A., & Sullivan, R. M. (2011). Cortical processing of odor objects. [Research Support, N.I.H., Extramural Review]. *Neuron*, *72*(4), 506-519. doi: 10.1016/j.neuron.2011.10.027

Figure Legends

Figure 1. Quantitative, high-throughput analysis of fos-IR across the brain. (a)

Nissl-stained reference image from the Allen Reference atlas – Version 1 (2008)

Specimen age P56, coronal level 68, bregma -1.3mm. (b) Histological section showing fos-IR at bregma -1.3mm, in a hindpaw menthol-stimulated wild-type animal. Scale bar: 1mm. Insets for B are representative template images of fos-IR cells used as training examples for automated cell detection. (c) Graph of fos-IR neurons counted in (b). (d)

Spatially averaged fos-IR for a single section to generate an activation map (~100x100 μm squares) for (b). (e) Same section as (b) at different contrast to show fidelity of cell counts at different contrast levels. (f) Spatially averaged fos-IR map for (E). (g) 3

sections from the same animal spanning 150 μm . (h) Averaged activation map generated from 3 aligned and analyzed tissue samples for fos-IR neurons from (g).

Figure 2. Optimizing peripheral TrpM8 activation: menthol stimulation on the hindpaw induces fos-IR in the dorsal horn.

(a) Schematic of mouse spinal cord indicating relative location of cervical (C1) thoracic (T1), lumbar (L1) and sacral (S1) areas. Forepaw-related sections were selected from ~C8-T1, hindpaw sections from ~L1-L5. (b) Representative image of fos-IR from a menthol (forepaw) unilaterally-stimulated (left side) cervical section. Contralateral, right-hand side represents the unstimulated side. (c) Same as (B) but for lumbar sections, after menthol stimulation of hindpaw. (d) Mean (\pm sem) fos-IR cells from stimulated and unstimulated (US) sides for menthol (green bars) and cold (blue bars) forepaw (FP; n=6 mice) and hindpaw (HP; n=6 mice) spinal cord sections. * indicate $p < 0.0001$ corrected for multiple comparisons.

Figure 3. Hindpaw menthol stimulation induces fos-IR across the brain. a-d)

Spatially-averaged fos-IR cells after menthol stimulation to the hindpaw in wild-type animals at 4 bregma locations. Animal numbers (n) and total number of tissue sections (m) were as follows: **(a)** n=5, m=9, **(b)** n=4 m=12, **(c)** n=6 , m=15, **(d)** n=6 m=17. **(e-h)**

As in A-D but after vehicle stimulation (70% ethanol). Animal numbers (n) and total number of tissue sections (m) were as follows **(e)** n=3 m=12, **(f)** n=4 m=12, **(g)** n=4 m=12, **(h)** n=4 m=12. **(i-l)** Nissl-stained reference images from corresponding bregma locations from Allen Reference atlas – Version 1 (2008).

Figure 4. TrpM8 knockouts show diminished menthol-evoked fos-IR . A-D)

Spatially-averaged fos-IR cells after menthol stimulation to the hindpaw in TrpM8 KO animals at 4 bregma locations. Animal numbers (n) and total number of tissue sections (m) were as follows: **(a)** n=2, m=6 , **(b)** n=3 m=9, **(c)** n=3, m=9, **(d)** n=3, m=9. **(e-h)**

Spatially-averaged fos-IR cells from hindpaw vehicle (70% ethanol)-stimulated TrpM8 knockout animals. Animal numbers (n) and total number of tissue sections (m) were as follows: **(e)** n=3, m=3 , **(f)** n=2 m=2, **(g)** n=3, m=3, **(h)** n=3, m=H. **(i-l)** Nissl stained reference images from corresponding bregma locations from Allen Reference atlas – Version 1 (2008).

Figure 5. Volatile menthol is sufficient to induce fos-IR in posterior insula, S2, piriform, and hypothalamus. (a-d)

Spatially-averaged fos-IR cells 500 mM from volatile menthol-stimulated wild-type animals at 4 bregma locations. **(a)** n=3, m=8, **(b)** n=3,m=8, **(c)** n=3, m=7; **(d)** n=3, m=6. **(e-h)** As in A but from volatile menthol-stimulated TrpM8 KO animals. **(e)** n=2, m=5, **(f)** n=2, m=5, **(g)** n=2, m=6, **(h)** n=2, m=5. **(i-l)** Nissl stained reference images from corresponding bregma locations from Allen Reference atlas – Version 1 (2008).

Figure 6. Statistical analysis of menthol-evoked fos-IR across activated brain

regions. (a) Nissl-stained reference section for location of ROIs for S1 (dotted area at top), piriform (dotted area at bottom left) and hypothalamus (dotted area at ventral

midline) for quantitative comparisons centered at bregma -0.4. (b) Nissl-stained section

for bregma -0.8, where no ROIs were selected. (c) Nissl-stained section for S2 ROI

centered at bregma -1.3. (d) Nissl-stained section for posterior insula ROI centered at

bregma -1.6. (e) Scatter plot of animal averages across four experimental groups for

selected ROIs. (f) Across-animal averages with statistical comparisons (one-way

ANOVA). Unless indicated, stimulation was confined to the hindpaw. Hypothalamus:

Asterisk indicates wildtype menthol-stimulated greater than other groups after Bonferroni

correction. S1 hindpaw: Asterisk indicated wildtype menthol-stimulated greater than

TrpM8 knock-out and volatile menthol-stimulated after Bonferroni correction. S2:

wildtype menthol greater than other groups after Bonferroni correction. Insula: wildtype

menthol-stimulated was different from wildtype vehicle-stimulated and TrpM8 knock-out

after Bonferroni correction. Volatile menthol was different from wildtype vehicle-

stimulated and TrpM8 knock-out after Bonferroni correction. Thus, both wildtype

menthol and volatile menthol-stimulated were both different from TrpM8 knock-out and

wildtype vehicle-stimulated. Piriform: wildtype menthol-stimulated was different from

TrpM8 knock-out menthol-stimulated, after Bonferroni correction.

Table 1. Primary and secondary antibodies used in the study

Antibody	Antibody ID or catalogue number	Antigen	Working dilution	Vendor
Anti-c-fos	PC38T (Ab-5) Rabbit polyclonal RRID AB_2314421	Synthetic peptide of amino acids 4–17 of human c-Fos	1:5000	Santa Cruz Biotechnology (note: this antibody is no longer commercially available)
Goat anti-rabbit AlexaFluor546	A-11035	Heavy and light chain of rabbit IgG, affinity purified	1:500	Life Technologies (now ThermoFisher)

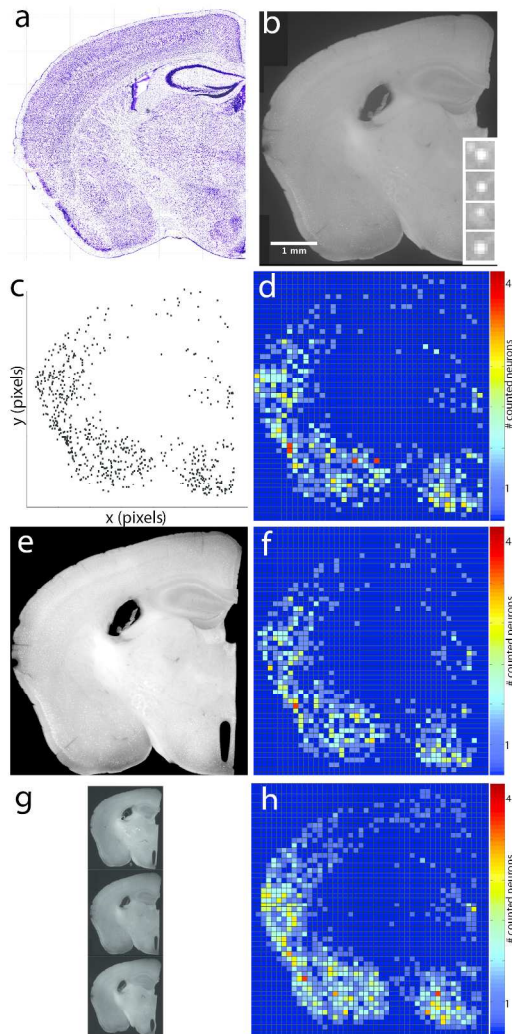


Figure 1. Quantitative, high-throughput analysis of fos-IR across the brain. (a) Nissl-stained reference image from the Allen Reference atlas – Version 1 (2008) Specimen age P56, coronal level 68, bregma -1.3mm. (b) Histological section showing fos-IR at bregma -1.3mm, in a hindpaw menthol-stimulated wild-type animal. Scale bar: 1mm. Insets for B are representative template images of fos-IR cells used as training examples for automated cell detection. (c) Graph of fos-IR neurons counted in (b). (d) Spatially averaged fos-IR for a single section to generate an activation map ($\sim 100 \times 100$ μm squares) for (b). (e) Same section as (B) at different contrast to show fidelity of cell counts at different contrast levels. (f) Spatially averaged fos-IR map for (E). (g) 3 sections from the same animal spanning 150 μm . (h) Averaged activation map generated from 3 aligned and analyzed tissue samples for fos-IR neurons from (g).

248x286mm (300 x 300 DPI)

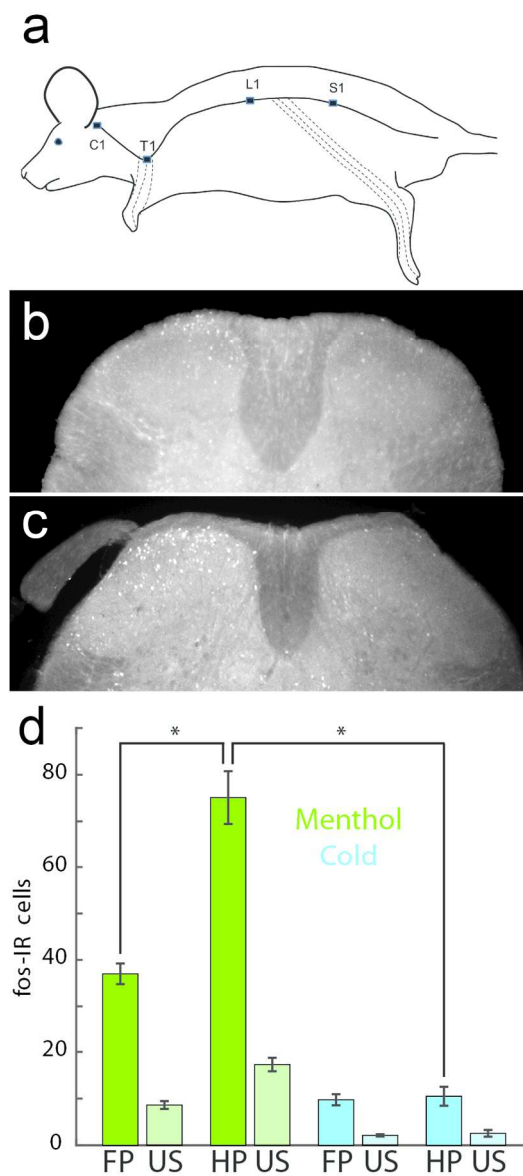


Figure 2. Optimizing peripheral TrpM8 activation: menthol stimulation on the hindpaw induces fos-IR in the dorsal horn.!! † (a) Schematic of mouse spinal cord indicating relative location of cervical (C1) thoracic (T1), lumbar (L1) and sacral (S1) areas. Forepaw-related sections were selected from ~C8-T1, hindpaw sections from ~L1-L5. (b) Representative image of fos-IR from a menthol (forepaw) unilaterally-stimulated (left side) cervical section. Contralateral, right-hand side represents the unstimulated side. (c) Same as (B) but for lumbar sections, after menthol stimulation of hindpaw. (d) Mean (+sem) fos-IR cells from stimulated and unstimulated (US) sides for menthol (green bars) and cold (blue bars) forepaw (FP; n=6 mice) and hindpaw (HP; n=6 mice) spinal cord sections. * indicate $p < 0.0001$ corrected for multiple comparisons.!! †

97x191mm (300 x 300 DPI)

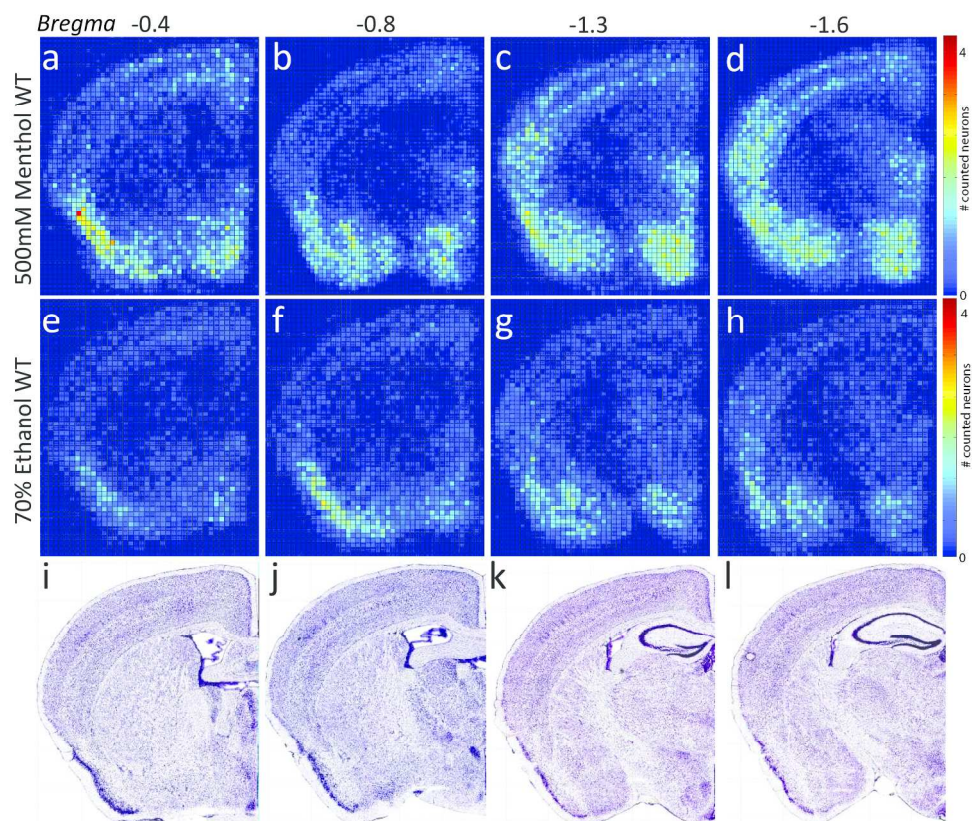


Figure 3. Hindpaw menthol stimulation induces fos-IR across the brain. a-d) Spatially-averaged fos-IR cells after menthol stimulation to the hindpaw in wild-type animals at 4 bregma locations. Animal numbers (n) and total number of tissue sections (m) were as follows: (a) n=5, m=9, (b) n=4 m=12, (c) n=6, m=15, (d) n=6 m=17. (e-h) As in A-D but after vehicle stimulation (70% ethanol). Animal numbers (n) and total number of tissue sections (m) were as follows (e) n=3 m=12, (f) n=4 m=12, (g) n=4 m=12, (h) n=4 m=12. (i-l) Nissl-stained reference images from corresponding bregma locations from Allen Reference atlas – Version 1 (2008).

211x179mm (300 x 300 DPI)

Acc

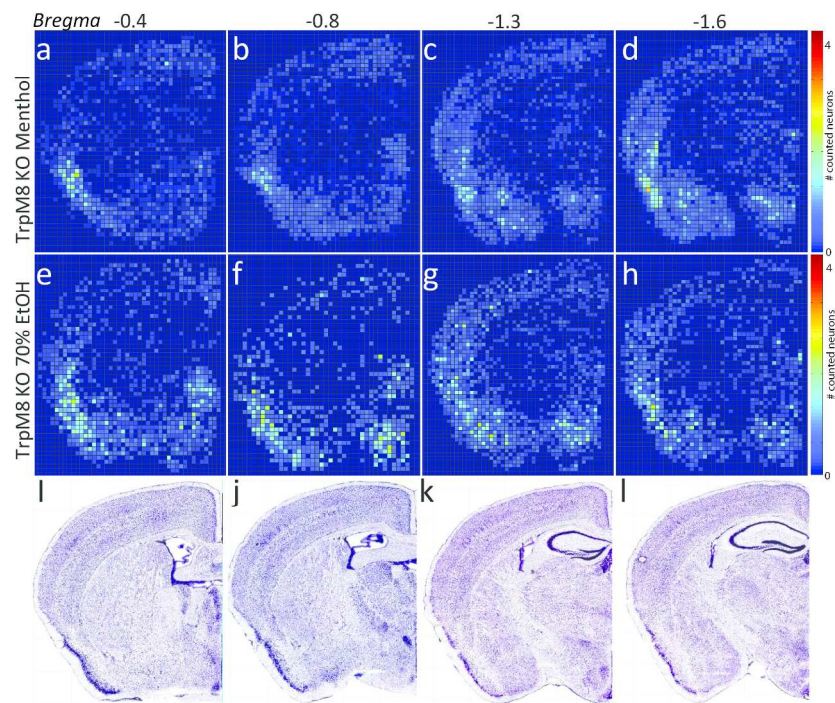


Figure 4. TrpM8 knockouts show diminished menthol-evoked fos-IR . A-D) Spatially-averaged fos-IR cells after menthol stimulation to the hindpaw in TrpM8 KO animals at 4 bregma locations. Animal numbers (n) and total number of tissue sections (m) were as follows: (a) n=2, m=6 , (b) n=3 m=9, (c) n=3, m=9, (d) n=3, m=9. (e-h) Spatially-averaged fos-IR cells from hindpaw vehicle (70% ethanol)-stimulated TrpM8 knockout animals. Animal numbers (n) and total number of tissue sections (m) were as follows: (e) n=3, m=3 , (f) n=2 m=2, (g) n=3, m=3, (h) n=3, m=H. (i-l) Nissl stained reference images from corresponding bregma locations from Allen Reference atlas – Version 1 (2008).

247x186mm (300 x 300 DPI)

Acce]]

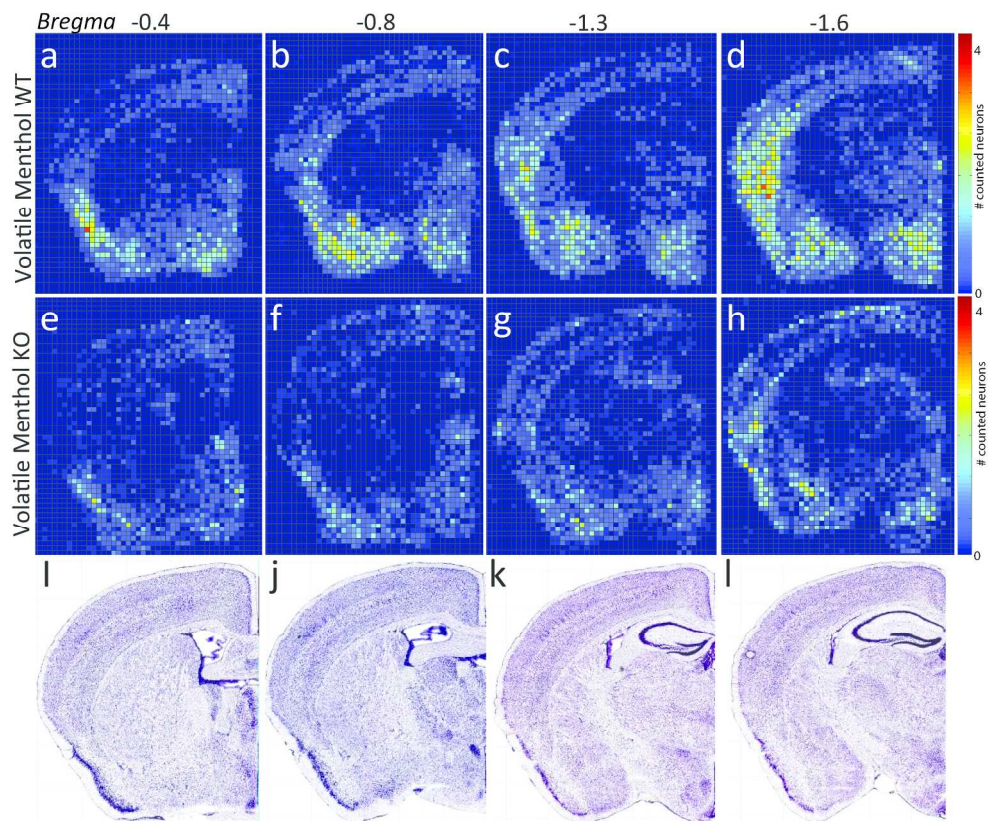


Figure 5. Volatile menthol is sufficient to induce fos-IR in posterior insula, S2, piriform, and hypothalamus. (a-d) Spatially-averaged fos-IR cells 500 μ m from volatile menthol-stimulated wild-type animals at 4 bregma locations. (a) n=3, m=8, (b) n=3, m=8, (c) n=3, m=7; (d) n=3, m=6. (e-h) As in A but from volatile menthol-stimulated TrpM8 KO animals. (e) n=2, m=5, (f) n=2, m=5, (g) n=2, m=6, (h) n=2, m=5. (i-l) Nissl stained reference images from corresponding bregma locations from Allen Reference atlas - Version 1 (2008).

211x179mm (300 x 300 DPI)

ACCE

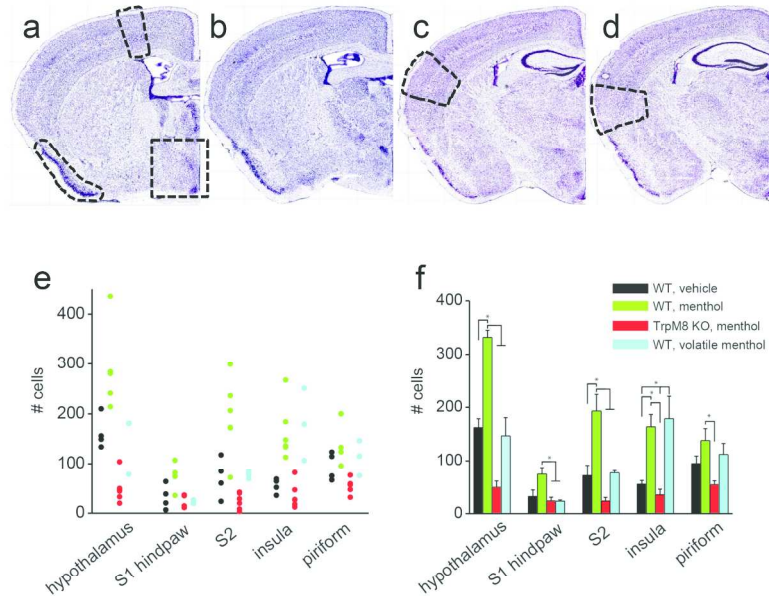
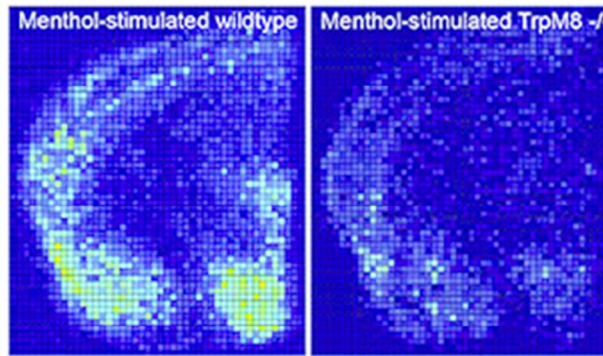


Figure 6. Statistical analysis of menthol-evoked fos-IR across activated brain regions. (a) Nissl-stained reference section for location of ROIs for S1 (dotted area at top), piriform (dotted area at bottom left) and hypothalamus (dotted area at ventral midline) for quantitative comparisons centered at bregma -0.4. (b) Nissl-stained section for bregma -0.8, where no ROIs were selected. (c) Nissl-stained section for S2 ROI centered at bregma -1.3. (d) Nissl-stained section for posterior insula ROI centered at bregma -1.6. (e) Scatter plot of animal averages across four experimental groups for selected ROIs. (f) Across-animal averages with statistical comparisons (one-way ANOVA). Unless indicated, stimulation was confined to the hindpaw. Hypothalamus: Asterisk indicates wildtype menthol-stimulated greater than other groups after Bonferroni correction. S1 hindpaw: Asterisk indicated wildtype menthol-stimulated greater than TrpM8 knock-out and volatile menthol-stimulated after Bonferroni correction. S2: wildtype menthol greater than other groups after Bonferroni correction. Insula: wildtype menthol-stimulated was different from wildtype vehicle-stimulated and TrpM8 knock-out after Bonferroni correction. Volatile menthol was different from wildtype vehicle-stimulated and TrpM8 knock-out after Bonferroni correction. Thus, both wildtype menthol and volatile menthol-stimulated were both different from TrpM8 knock-out and wildtype vehicle-stimulated. Piriform: wildtype menthol-stimulated was different from TrpM8 knock-out menthol-stimulated, after Bonferroni correction.

254x190mm (300 x 300 DPI)

AC

TrpM8-mediated somatosensation in mouse neocortex



141x105mm (72 x 72 DPI)

Accepted

Accepted Article

Activation of cutaneous TrpM8 receptor-expressing neurons was used to identify candidate neocortical areas responsive for cool sensation. Brain areas corresponding to the posterior insular cortex and secondary somatosensory (S2) show elevated fos-IR after menthol stimulation, with weaker activation in primary somatosensory cortex (S1). Menthol-mediated activation was absent in TrpM8-knock-out animals. Our results indicate that cool somatosensory input broadly drives neural activity across the mouse brain, with neocortical signal most elevated in the posterior insula, as well as S2 and S1.